Shapes of clusters and groups of galaxies: Comparison of model predictions with observations

D. J. Paz[1,2] ⋆, D. G. Lambas[1,2], N. Padilla[3], M. Merchán[1,2]

[1] *Grupo de Investigaciones en Astronomía Teórica y Experimental (IATE), Observatorio Astronómico de Córdoba, UNC, Argentina.*
[2] *Consejo Nacional de Investigaciones Científicas y Tecnológicas (CONICET), Argentina.*
[3] *Departamento de Astronomía y Astrofísica, Pontificia Universidad Católica, V. Mackenna 4860, Casilla 306, Santiago 22, Chile.*
⋆ *e-mail: dpaz@oac.uncor.edu*

5 February 2008

ABSTRACT
We study the properties of the 3-dimensional and projected shapes of haloes using high resolution numerical simulations and observational data where the latter comes from the 2PIGG (Eke et al. 2004) and SDSS-DR3GC group catalogues (Merchán & Zandivarez 2005). We investigate the dependence of halo shape on characteristics such as mass and number of members. In the 3-dimensional case, we find a significant correlation between the mass and halo shape; massive systems are more prolate than small haloes. We detect a source of strong systematics in estimates of the triaxiality of a halo, which is found to be a strong function of the number of members; ΛCDM haloes usually characterised by triaxial shapes, slightly bent toward prolate forms, appear more oblate when taking only a small subset of the halo particles.
The ellipticities of observed 2PIGG and SDSS-DR3GC groups are found to be strongly dependent on the number of group members, so that poor groups appear more elongated than rich ones. However, this is again an artifact caused by poor statistics and not an intrinsic property of the galaxy groups, nor an effect from observational biases. We interpret these results with the aid of a GALFORM mock 2PIGG catalogue. When comparing the group ellipticities in mock and real catalogues, we find an excellent agreement between the trends of shapes with number of group members. When carefully taking into account the effects of low number statistics, we find that more massive groups are consistent with more elongated shapes. Finally, our studies find no significant correlations between the shape of observed 2PIGG or SDSS-DR3GC groups with the properties of galaxy members such as colour or spectral type index.

Key words: large-scale structure of Universe, methods: N-body simulations, galaxies: kinematics and dynamics cosmology: theory

1 INTRODUCTION

Cluster and groups of galaxies provide invaluable information on the formation and evolution of structure in the Universe. These systems, also denominated haloes, represent the largest gravitationally bound systems in the universe. It has been shown that these systems are mildly aspherical with orientations related to the surrounding structures such as filaments and large scale walls (see Kasun & Evrard, 2005, and references therein). Results from numerical simulations by van Haarlem & van de Weygaert (1993, see also Splinter et al., 1997) have shown that the origin for such alignments comes from re-arrangements of the halo axes in the direction of the accretion anisotropy (e.g. last major merger event). Therefore, in a statistical sense, the shapes of haloes could

encode information about the large-scale structure in the Universe. On the other hand, current halo models (Cooray & Sheth, 2002, van den Bosch et al. 2004), which successfully describe several galaxy statistics, assume that the distribution of mass in haloes is spherical. However, a more accurate version of the model would need to take into account the actual complicated internal structure (Jing & Suto, 2002), and aspherical shapes of haloes.

Halo properties have been studied extensively using numerical simulations. For instance, high resolution, but relatively small volume simulations have been used to provide detailed information on the halo density profile and halo shape, whereas larger volume, but low resolution simulations (e.g. the Hubble Volume simulations, Evrard et al.

2002) have provided information on the abundance and spatial distribution of haloes (Colberg et al., 1999, ,Colberg et al. 2000, Jenkins et al., 2001, Padilla & Baugh, 2002).

Several authors (Warren et al., 1992, Thomas et al., 1998, Hopkins, Bahcall & Bode, 2005, Kasun & Evrard, 2005, and references there in) have analysed the distribution of halo shapes using the best fitting ellipsoid to the spatial distribution of halo members. They calculate the minor to major semi-axis ratio of each halo, and use it as an indicator of the best-fitting ellipsoid shape. In order to obtain reliable distributions of semi-axis ratios, it is necessary to reach an equilibrium between spatial resolution (to improve the estimate of semi-axis ratios) and comoving volume (for good statistics). Kasun & Evrard (2005) combine large volume and high resolution simulations, to find a systematic trend with halo shape: a larger ratio of minor to major semi-axes is obtained when larger halo masses are considered. These authors also find good alignments between velocity and spatial principal semi-axes. Furthermore they find that cluster shapes are independent of environment and reflect the filamentary structure of the universe through a non-random alignment at very large scales of up to 200 h^{-1} Mpc.

On the observational side, Plionis, Basilakos, & Tovmassian (2004) find a trend of shape with cluster size that is opposite to that seen in simulations (Kasun & Evrard, 2005). From 1168 groups in the UZC-SSRS2 galaxy group catalogue, Plionis et al. concluded that poor groups are more elongated than rich ones, with 85% of poor groups having a projected semi-axis ratio lower than 0.4.

In this work, we explore shapes of dark matter haloes with masses ranging from groups to clusters of galaxies using a high resolution cosmological simulation with a modest volume ($250^3 h^{-3} Mpc^3$). We analyse the dependence of triaxiality, asphericity and projected shape on group mass, and number of members. By studying observational samples of groups from the 2PIGG (Eke et al. 2004, constructed from the 2-degree Field Galaxy Redshift Survey, Colless et al. 2001) and the SDSS-DR3GC group catalogue (Merchán & Zandivarez, 2004, constructed using the Data Release 3 of the Sloan Digital Sky Survey, SDSS-DR3, Abazajian et al., 2004), we will demonstrate that the apparent inconsistency between the observational and simulated groups is mainly due to an artifact produced by low number statistics. To study this apparent discrepancy we combine three-dimensional and two-dimensional analyses performed over a numerical simulation box and a mock catalogue, respectively. In both cases the cosmology corresponds to a standard ΛCDM model. In addition, when constructing the mock catalogue, we make use of the GALFORM (Cole et al. 2000) semi-analytic galaxies populating the simulation box. In particular, the mock catalogue provides us with an excellent test sample to explore the outcomes of group and cluster shape measurements within the current cosmological context.

This paper is organised as follows. In section 2 we provide a study of 3-dimensional shapes of haloes in the numerical simulation, including analyses of systematic biases coming from low number statistics. Section 3 contains a study of projected group shapes from observational datasets, and provides a theoretical framework to interpret our results by means of a mock group catalogue and the projection onto
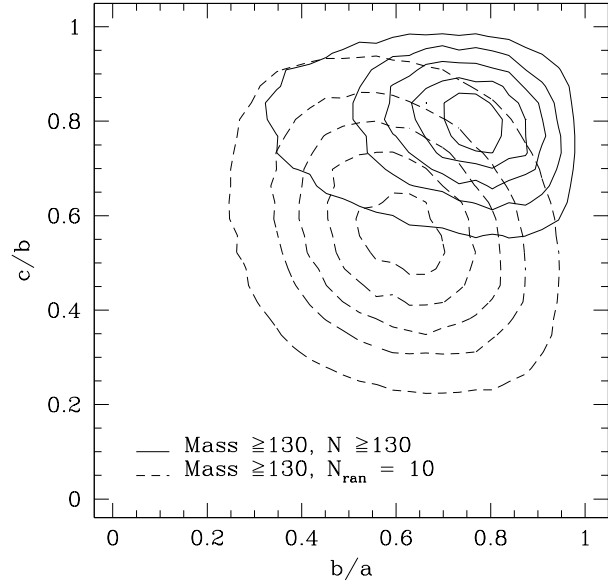

Figure 1. Contour maps of the scatter-plot of b/a vs. c/b semi-axis ratios (see text) for groups with masses $M > 10^{12} M_\odot$. Solid lines correspond to the values estimated using all members, while dashed lines show b/a vs. c/b when only 10 random group members are used in the calculation. Contours enclose 10, 30, 50, 70, and 90% of the b/a vs. c/b points (inner to outer contours, respectively).

two dimensions of the 3-dimensional haloes in the simulation. Finally, we summarise the main conclusions from this work in section 4.

2   3-DIMENSIONAL ANALYSIS

In this section we analyse the predicted shape of gravitationally bound systems with masses ranging from groups to clusters of galaxies ($10^{12} h^{-1} M_\odot$ to $10^{15} h^{-1} M_\odot$). These systems were taken from a cosmological numerical simulation kindly provided by the Durham group, performed using the first version of the GADGET code developed by Springel et al. (2001). The computational volume corresponds to a periodic box of side $250 h^{-1}$Mpc containing 500^3 particles with masses $M = 1.04 \times 10^{10} h^{-1} M_\odot$. The simulation adopts a Cold Dark Matter (CDM) model with density parameters $\Omega_0 = 0.3$, $\Omega_\Lambda = 0.7$, and a present rms mass fluctuations of $\sigma_8 = 0.8$. The identification of clumps of particles is carried out by means of a standard friends-of-friends algorithm, with a percolation length of $l = 0.17 n^{-1/3}$, were n is the mean number density. We only consider haloes with at least 10 particles.

2.1   Shapes of Halos

For each dark-matter halo, we calculate the inertia tensor using positions of halo members. This can be written as a symmetric matrix,

$$I_{ij} = (1/N_h) \sum_{\alpha=1}^{N_h} X_{\alpha i} X_{\alpha j}, \qquad (1)$$

where $X_{\alpha i}$ is the ith component of the displacement vector of a particle α relative to centre of mass, and N_h is the number of particles in the halo. The matrix eigenvalues correspond to the square of the semi-axis (a, b, c were $a > b > c$) of the characteristic ellipsoid that best describes the spatial distribution of the halo members. Our group shape analysis is based on the semi-axis ratios b/a and c/b. These variables are independent and provide a complete set of parameters to analyse the ellipsoid shape. Several authors use the quotient of minor to major eigenvalues (c/a), since this ratio provides more appreciable changes with the ellipsoid asphericity. However, such a parameter does not discern between oblate and prolate ellipsoids. Figure 1 shows the contour map of the scatter plot of b/a vs c/b ratios for groups with masses $M > 10^{12} M_\odot$ (solid lines containing 10, 30, 50, 70, and 90% of the b/a vs. c/a pairs). Here a fixed $b/a = 1$ with an arbitrary value of c/b, corresponds to perfect oblate ellipsoids. On the other hand, systems with fixed $c/b = 1$ are perfect prolate ellipsoids. A system with $b/a < c/b$ is associated to a general triaxial ellipsoid with prolate tendency, while the opposite case, $b/a > c/b$, corresponds to a predominantly oblate ellipsoid. As can be seen, haloes are generally triaxial; their shapes are almost uniformly distributed between the two extremes (inner contours) with a slight preference (outer contours) to prolate configurations (i.e. $a \gg b > c$). The most frequent values of semi-axis ratios are $c/b = 0.8$ and $b/a = 0.76$. This is in qualitative agreement with Frenk et al. (1998) but with much higher statistical significance.

2.2 Resolution Effects in the determination of halo shapes

When using galaxy catalogues and low resolution simulations, only a few group members are available to estimate the inertia tensor. We therefore study possible low number effects in the estimate of semi-axis ratios. There are two main effects expected to take part in biasing the distribution of shapes. On the one hand, semi-axes of similar amplitude will be affected by shot noise due to the use of a small number of discrete particles when calculating the inertia tensor. This will induce a rearrangement of the semi-axes resulting in smaller c/b and b/a semi-axis ratios. On the other hand, the inertia tensor is a second order measure, which implies that a further, more complicated bias is to be expected. We test these hypotheses by computing halo semi-axis ratios using only a subsample of randomly selected halo members. Figure 1 (dashed lines) shows iso-density contours of b/a vs. c/b ratios determined using 10 randomly selected particles. When comparing with the results obtained using all the halo particles it can be noticed that the shape parameters from all members have been shift towards lower c/b and b/a values, in agreement with our first hypothesis. In addition, it can be seen that the degradated distribution is shifted toward more oblate values with a peak density at lower b/a and c/b ratios. We identify this systematic effect with our second source of biases. The reason for this phenomenon could reside in the fact that shot noise can only reduce the signal (ie. by definition: $b/a < 1$ and $c/b < 1$), which makes the smaller semi-axis more prone to be affected by noise. Therefore, prolate shapes (two small semi-axis) are more distorted by noise than oblate shapes (only one small semi-axis).
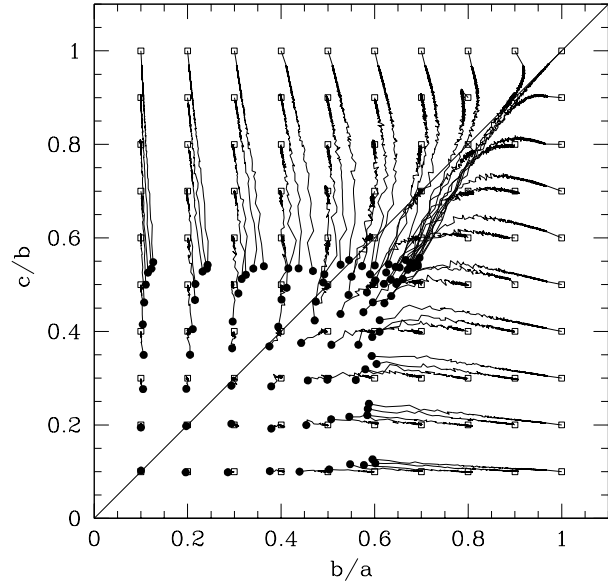

Figure 2. Dependence of semi-axis ratio estimates (b/a and c/b) on the number of randomly selected points used to calculate the inertia tensor (solid lines). The open squares are the set values in each Monte-Carlo ellipsoid; the filled circles represent the values obtained using sets of five randomly extracted points from each Monte-Carlo ellipsoid.

To probe quantitatively these concepts, we perform a Monte-Carlo simulation and homogeneously cover the parameter space (b/a, c/b) with ellipsoids populated with 10,000 points, and calculate average semi-axis ratio estimates, determined using sets of different numbers of randomly selected ellipsoid points. Figure 2 shows the path (solid lines) described by the ellipsoid shapes as the number of members used to calculate the inertia tensor (hereafter N_{ran}) is reduced from 1000 to 5. The open squares show the underlying values for each Monte-Carlo ellipsoid. The filled circles show the results when only five randomly extracted points are used to calculate b/a and c/b. As we have mentioned previously, the effect of the low number statistics is to produce a systematic displacement to lower values of b/a and c/b, with a stronger effect on spherical shapes with a tendency to populate the oblate region.

2.3 Shape dependence on cluster mass

The analysis in the previous section showed that haloes are preferentially prolate. Previous works (Kasun & Evrard, 2005, Jing & Suto, 2002) are consistent with a weak dependence of the mean c/a parameter on mass, which is commonly used to indicate the asphericity of a dark-matter halo. In order to provide a suitable characterization of the shape dependence on mass and number of particles, we introduce a new parameter that allows us to differentiate between prolate and oblate ellipsoids, which we find more suitable to perform the task than the c/a ratio. A simple way to define this parameter, is to calculate the quotient between the parameters c/b and b/a; prolate systems satisfy $ca/b^2 > 1$,
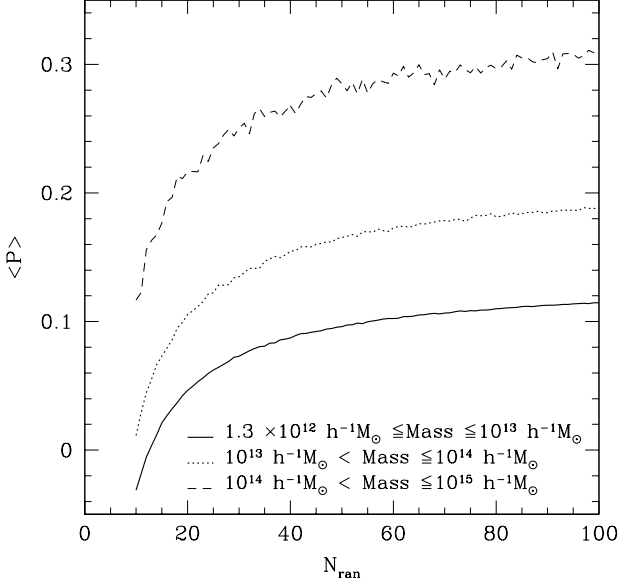
Figure 3. The evolution of the triaxiality parameter P with N_{ran} for ranges of increasing halo mass (solid, dotted, and dashed lines respectively).

whereas oblate systems, $ca/b^2 < 1$. Consequently we define the triaxiality parameter as:

$$P := \ln(ca/b^2). \tag{2}$$

Using the logarithm avoids the natural skewness of the ca/b^2 distribution, arising from the asymmetry between the oblate $(0 < ca/b^2 < 1)$ and prolate $(1 < ca/b^2 < \infty)$ parameter ranges. Therefore an oblate (prolate) ellipsoid satisfies $P < 0$ $(P > 0)$. Regardless of the number of particles used to calculate the inertia tensor, we find a dependence of the distribution of cluster shapes on mass consistent with previous determinations. Figure 3 shows the triaxiality parameter as a function of number of particles N_{ran} for different mass ranges. In spite of the tendency of increasing values of P with N_{ran} (which reflects the number effect described in the previous section) curves corresponding to different mass ranges are well separated indicating the triaxiality dependence on cluster mass regardless of N_{ran}.

In Figure 4 we show the dependence of the mean values of the triaxiality parameter P (left panel) and c/a ratio (right panel) on mass. Error bars correspond to the standard *rms* error in P and c/a. Consistent with the results for c/a obtained by Kasun & Evrard (2005) and Jing & Suto (2002), we find a decreasing log-linear relation between the c/a ratio and halo mass (i.e. the asphericity increases). We also find that P increases with mass, indicating that the increment in asphericity comes from an increased prolaticity in the halo population. The fitting formulae shown by the solid lines correspond to,

$$< c/a > = -(0.056 \pm 0.003)\log_{10}(M) + (0.70 \pm 0.01), \tag{3}$$

$$< P > = (0.089 \pm 0.005)\log_{10}(M) - (0.11 \pm 0.01). \tag{4}$$

The trend in c/a is significantly more ellipsoidal than the results from Kasun & Evrard (2005), but as was pointed out by these authors in relation to the work by Thomas et al. (1998), the reason for such discrepancies lies in the definition of halo shape. The boundary constraint of the spherical over-density method used by these authors to identify haloes, tends toward rounder measures of the inertia moments, whereas our haloes tend to be more elongated due to the directional nature of the percolation process and the pruning in local density. As will be shown later in this work, the trend in projected semi-axis ratios with mass is that of more elongated shapes for more massive haloes.

The results obtained in this section indicate that even though there is a clear tendency in triaxiality and asphericity with halo mass, statistical biases coming from the number of halo members used to calculate the halo shape, must be carefully considered. Our analyses suggest that in order to obtain a reliable dependence of halo shape properties with mass one should consider using a fixed number of halo members regardless of halo mass. This can certainly result in a systematic off-set in the shape-mass relation, but will allow the detection of any underlying trend with mass.

3 PROJECTED ANALYSIS

Due to redshift distortions, the analysis of observational data from redshift surveys is limited to the measurement of group shapes as seen projected on the plane of the sky. Therefore, when studying observational samples of groups, we estimate projected shapes following a similar procedure to the one described for the 3-dimensional case. Using the projected Cartesian coordinates on the plane of the sky, we calculate the 2-dimensional inertia tensor, whose eigenvalues provide the semi-axes a and b (major and minor semi-axes, respectively). In this work we analyse the projected shapes of groups in the 2PIGG (2dFGRS Percolation Inferred Galaxy Groups), constructed from the full 2-degree Field Galaxy Redshift Survey (2dFGRS) by Eke et al. (2004), and in the group catalogue compiled by Merchán & Zandivarez (2005) from the Data Release 3 of the Sloan Digital Survey (SDSS-DR3GC). The 2PIGG catalogue contains $4,045$ groups with at least 4 members, and the SDSS-DR3GC group catalogues, $10,152$ groups. In order to compare observational and numerical simulation results we construct a mock 2dFGRS catalogue by placing an observer at random within the simulation box, and reproducing as many of the 2dFGRS observational biases as possible. This is done by placing the same angular completeness mask and selection function as in the real 2dFGRS survey, and by measuring the distances to galaxies using redshifts instead of coordinate distances (For more details on 2dFGRS mock construction see Eke et al., 2004). The galaxies in the mock catalogues correspond to GALFORM semi-analytic galaxies populating the numerical simulation already described in earlier sections. After generating the mock galaxy catalogue, we apply the group finding algorithm originally used to identify the group catalogues in the real data, namely the Eke et al. (2004) Friends-of-Friends (FOF) algorithm to the 2dFGRS mock catalogue (software kindly provided by Vincent Eke).
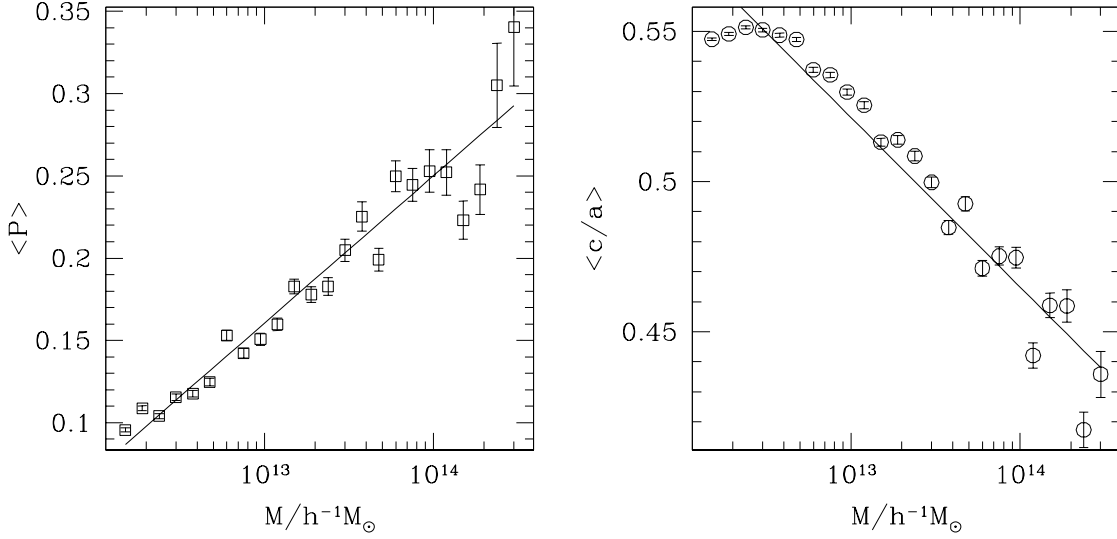
Figure 4. Triaxiality parameter P, and c/a ratios as a function of halo mass (symbols in left and right panels respectively). The lines show the best fitting log-linear relations to the measurements from the numerical simulation (Equations 3 and 4.)

3.1 Dependence of group shape on number of members

The study of halo shapes in the numerical simulation shows that results can change dramatically when different numbers of halo members are used to infer the halo shape. In this section we will assess the importance of this effect when calculating the 2-dimensional inertia tensor of groups identified from a galaxy redshift survey.

In order to do this, we proceed to calculate the shapes of groups in the real and mock 2PIGG catalogues and compute the distribution of shapes for different numbers of group members, N_{gal}. We show the results from this calculation in Figure 5. As can be seen, there is a striking resemblance between the results from mock and real data. For instance, in both cases the distribution obtained from groups with $N_{gal} \geq 4$ corresponds to more elongated projected shapes than that corresponding to $N_{gal} \geq 20$. The agreement for different values of N_{gal} between data and mock groups is excellent, specially for the low N_{gal} samples. This indicates that the Cole et al. (2000) model is adequate for this comparison. It is also interesting to observe the apparent increase of the typical semi-axis ratio with the number of group members. As we will later demonstrate, this observed trend is mainly due to low number statistics. The same figure also shows the results for groups in the SDSS-DR3GC, which are in excellent agreement with mock and real 2PIGG group shapes. This is a good indication of the robustness of our results, since the group identification algorithms used in the 2PIGG and SDSS-DR3GC group catalogues are slightly different, the catalogues cover different areas on the sky, have slightly different depths, and suffer from very different observational biases due to the instrument setups used in the construction of the surveys (see Colless et al., 2001, for the 2dFGRS and Abazajian et al., 2004, for the SDSS-DR3).

The increase in the average values of b/a with the number of group members seen in Figure 5, is in agreement with
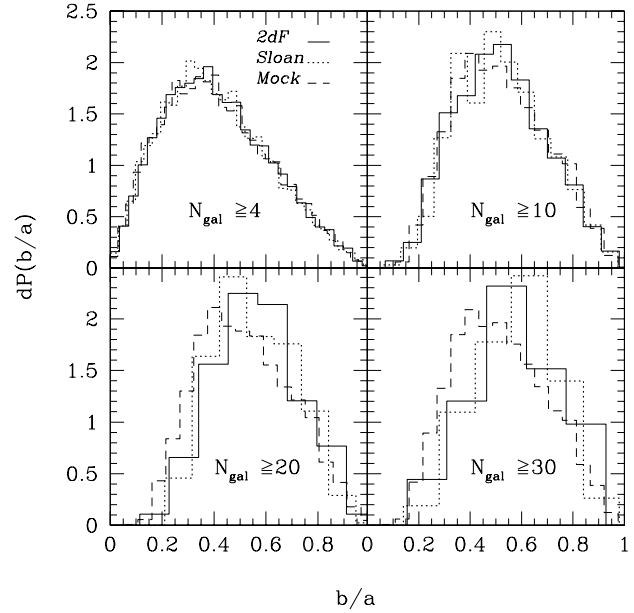

Figure 5. Distributions of b/a for the 2PIGG (solid lines), mock 2PIGG (dashed lines) and SDSS-DR3GC (dot-dashed lines) groups, for different ranges of N_{gal} (different panels, see figure keys).

the study of Plionis et al. (2004) of the UZC-SSRS2 groups (see above). There have been suggestions for explaining the variation in typical group shapes with N_{gal}, such as mechanisms for the accretion of matter which would depend on the halo mass, or dynamical friction (Plionis et al., 2004). However, studies of haloes in numerical simulations seem to point in the opposite direction (Section 2, this work, Kasun & Evrard, 2004, Hopkins et al., 2005), which poses a controversy between theory and observations. A solution to this discrepancy was proposed by Kasun & Evrard (2004),

whereby the optical selection of galaxies would be responsible for important biases that would reverse the dependence of halo shape on mass.

We now search for the reason behind the increase in the typical projected semi-axis ratio with the number of group members, N_{gal}. Our results from the study of halo shapes in the numerical simulation have shown that the use of a low number of halo members tends to lower the halo tri-axiality parameter in a systematic way (see Section 2). We apply the same procedure to the observational data, and compare the distribution of semi-axis ratios for groups with $N_{gal} = 6$ to the distribution measured from groups with $N_{gal} \geq 20$ members but only considering 6 randomly selected galaxies from each group (for example, out of a group with 20 members, one can select 38760 subgroups of 6 members each; we present our results from calculating the shapes of only 200 subgroups per individual group with $N_{gal} > 19$, this number of subgroups ensures statistical independence to some degree). Figure 6 shows the distribution of group semi-axis ratios with low values of $N_{gal} = 6$ (long-dashed histogram) and compares it to the distribution of groups with $N_{gal} > 19$ resulting from using all the group members (solid histogram; again, groups with larger number of members are consistent with rounder projected shapes) and when selecting only 6 members for measuring their shapes (dot-dashed histogram). It is clear from this figure that the distribution of group shapes with $N_{gal} = 6$ is indistinguishable from that of richer groups where only 6 members are considered when measuring their shapes (apparently more elongated than when using all the group members). The latter distribution is very smooth due to the large number of subgroups considered. Therefore, we can conclude that the trend of shape with the number of group members is mainly due to a systematic effect, and that it may very well be possible that intrinsic group shapes do not vary significantly with the number of group members.

Based on these results, we provide a measurement of an unbiased distribution of group shapes from groups with any number of members (bearing in mind that any dependence of the group shape on mass will be averaged out in this analysis). In order to do this, we generate samples of subgroups with numbers of members ranging from 4 to 16, extracted from a sample of groups with $N_{gal} > 19$ (200 subgroups from each group), and calculate the distribution of shapes for the subgroups of different numbers of members. We fit a 4th order polynomial to the result using N_{ran} extracted members,

$$F_{N_{ran}}(b/a) = \sum_{i=0}^{4} h_i (b/a)^i. \qquad (5)$$

We then define correction factors which can be applied to the distributions of semi-axis ratios of groups with N_{gal} members, and make these measurements equivalent to what would result from using ≥ 20 members instead of N_{gal},

$$C_{N_{gal}}(b/a) = F_{\geq 20}(b/a)/F_{N_{ran}=N_{gal}}(b/a), \qquad (6)$$

where $F_{\geq 20}$ is the fit to the measured distribution of groups with $N_{gal} \geq 20$ members. Note that the correction factors are obtained from the same sample of groups to which these will be applied. We show in Figure 7 the resulting corrected distributions of semi-axis ratios for N_{gal} ranging from 4 to
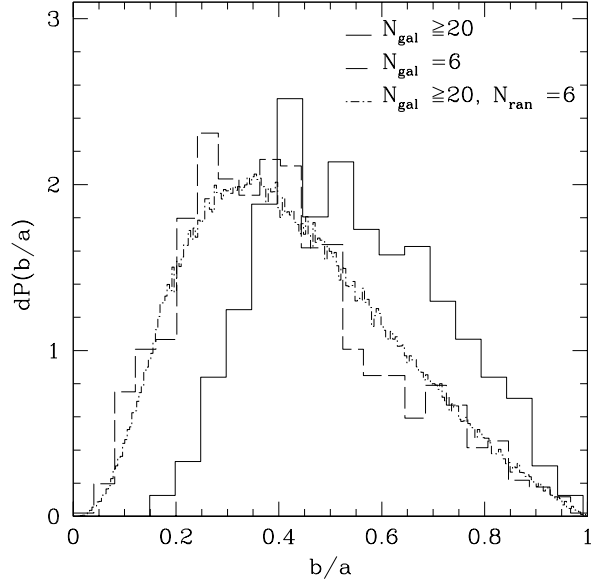

Figure 6. Distribution of projected semi-axis ratios b/a from groups with $N_{gal} = 6$ (dashed lines), groups with $N_{gal} > 19$ (solid lines) and groups with $N_{gal} > 19$ where only 6 group members were used to obtain the group shape (dot-dashed lines).

13. As can be seen, the corrected distributions for different N_{gal} show some uncorrelated scatter around a single distribution that can be fitted by a fourth order polynomial. For the 2PIGG catalogue, the best fitting coefficients are $h_0 = 0.22 \pm 0.07$, $h_1 = -7 \pm 1$, $h_2 = 37.9 \pm 4.5$, $h_3 = -49 \pm 7$, and $h_4 = 19.5 \pm 3$. As can be seen in this figure, the best fit polynomials corresponding to the results from the 2PIGG, mock 2PIGG and SDSS-DR3GC groups are extremely similar.

3.2 Dependence of group shapes on mass

In order to avoid systematic trends in the shapes of haloes, we devise a simple statistical method that will unveil any shape dependence on mass in the observational data.

As a first step to provide a connection between the results from the 3-dimensional shapes of haloes in the full simulation box we simply project onto two dimensions a sample of haloes taken from the simulation. This sample is characterised by the same mass distribution present in the 2PIGG catalogue, ensuring the study of similar samples of groups from the simulation and the data. The masses of 2PIGG groups are calculated using group luminosities and a M/L relation from Eke et al. (2004). To achieve a realistic shape comparison, the number effect is also taken into account by forcing the same distribution of number of members present in the 2PIGG catalogue (we do this by randomly selecting members from each group in the simulation). The distributions of projected semi-axis ratios b/a of this particular halo sample (solid line) and the mock 2PIGG catalogue (doted line) are shown in Figure 8. As can be seen, both distributions are in reasonably good agreement. However, mock groups show a weak tendency to be more elongated than those obtained by direct projection of the simulations. Even though this effect is small, we find that it persists even when
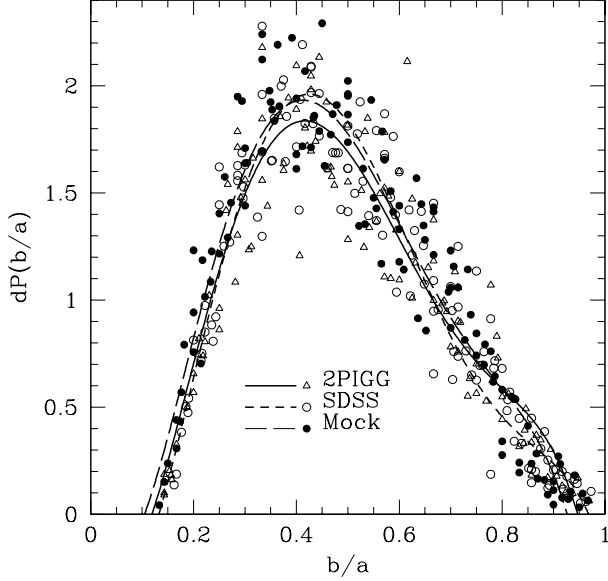
Figure 7. Distributions of projected b/a semi-axis ratios corrected to an equivalent of $N = 20$ group members used for computing the group shapes. Results are shown for the 2PIGG, mock 2PIGG and SDSS-DR3GC catalogues (see the figure key).

Figure 8. b/a distributions of projected 3-dimensional haloes (solid line) and of mock groups (doted line). The distributions of 3-d halo mass and number of member distributions have been matched to those of the mock group sample.

sampling different ranges of mass and number of members. Therefore, it is possible that the offset shown by both distributions is due to differences between the identification algorithms used on simulations and redshift-space samples. For instance, the latter algorithms use a complicated linking volume, characterised by an assumed angular to radial aspect ratio, and a scaling with redshift (see Eke et al., 2004, for more details). This comparison could be adopted in future works as a further test for assessing the quality of identification algorithms applied to redshift data.

As previously mentioned, a good way to avoid the number effect on our statistics is to use a fixed number of group members to calculate the group shapes. We therefore compute the average b/a ratios of projected dark-matter haloes as a function of halo mass, using only 10 halo members out of the total available particles in each halo. The resulting semi-axis ratios can be seen in Figure 9, where more massive haloes are consistent with slightly more elongated shapes than less massive haloes (open circles). By comparing this trend with halo mass with what is obtained using all the halo particles for haloes with more than 100 members, we find only a constant systematic shift between the two. This indicates that the procedure of selecting only 10 halo members preserves the trend of projected shape with mass. We now proceed to calculate the average b/a ratios of groups in the mock 2PIGG catalogue, for all groups with at least 10 galaxy members, but using only 10 randomly selected members to calculate the group shape. We plot this result as a function of group mass, calculated using the M/L ratio characterising the mock catalogue (open squares). As can be seen, the trend with mass is recovered in the mock catalogue. Finally, we repeat this procedure using the real 2PIGG catalogue, and show the results in filled triangles (groups with at least 10 galaxy members, using only 10 members to measure b/a). It is clear from the figure, that
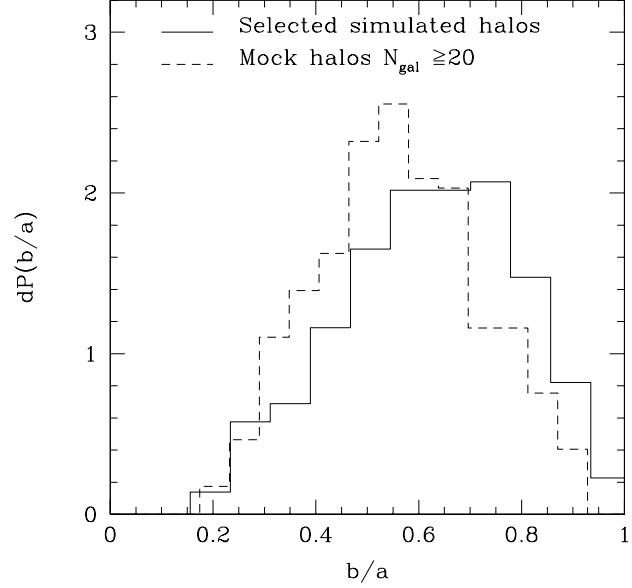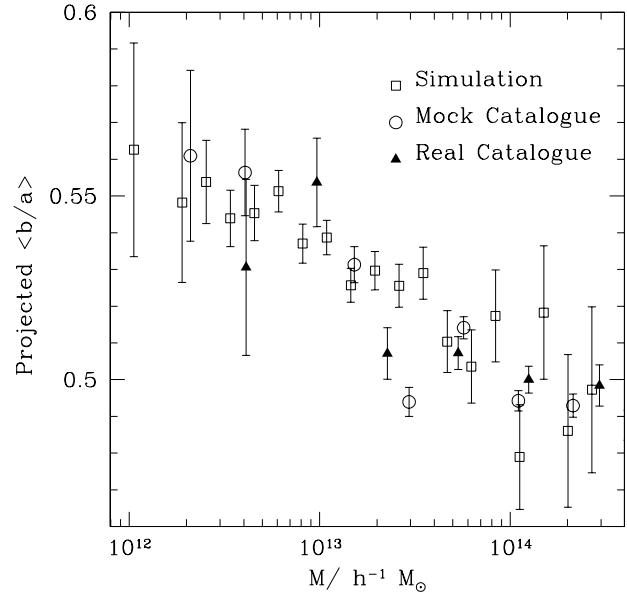

Figure 9. Dependence of average b/a ratios as a function of mass for haloes from the numerical simulation (circles), groups from the 2PIGG mock and real catalogues (squares and triangles, respectively). In all cases, only 10 randomly selected group members were used when calculating the projected group shape.

we have been able to reconcile the results from numerical simulations with those from observational data, as the 2PIGG groups show slightly more elongated shapes for massive systems ($b/a \simeq 0.53 \pm 0.023$ for $M = 4\ 10^{12} h^{-1} M_\odot$ and $b/a \simeq 0.49 \pm 0.06$ for $M = 2\ 10^{14} h^{-1} M_\odot$, implying a $1 - \sigma$ detection of a trend).
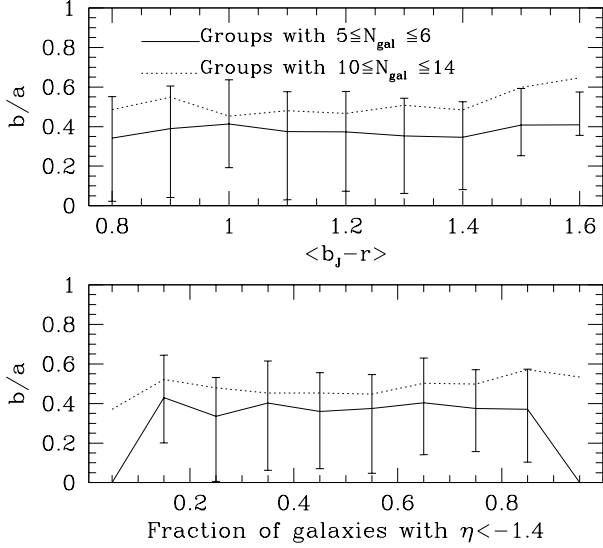
Figure 10. Dependence of average b/a ratios as a function of average $b_J - r$ colour (top panel) and fraction of group members with $\eta < -1.4$ (bottom panel) for 2PIGG groups. Solid lines (dotted lines) show the results for groups with $5 \leq N_{gal} \leq 6$ ($10 \leq N_{gal} \leq 14$). Error-bars correspond to the 10 and 90 percentiles.

3.3 Dependence of group shape on group member properties

We now search for possible differences in the typical shapes of groups when considering different properties of their galaxy members. We divide our samples of groups according to the average member galaxy colour and galaxy spectral type, since these can be considered indicators of different stellar formation rate histories and merger or interaction activity within the groups. In all comparisons, we ensure the same number of members is considered when measuring group shapes.

In general, we find that it is quite difficult to assess whether a correlation between shape and colour is detected in either the SDSS-DR3GC or 2PIGG catalogues. In particular, we present the results for the 2PIGG groups in the top panel of figure 10, where we show the median b/a as a function of $b_J - r$ colour, for two different ranges of number of group members N_{gal} (note the low number statistics effect inducing overall lower median b/a values for the lower N_{gal} case). We repeat this analysis using the spectral type index η (an indicator of the star formation activity in galaxies) in 2dFGRS galaxies, determining the fraction of member galaxies that satisfy $\eta < -1.4$ in each group. As can be seen in the bottom panel of figure 10, we again find no clear dependence of the average semi-axis ratios with the fraction of passively star forming galaxies within the group. In the case of SDSS-DR3GG groups, we perform this analysis using the e-class spectral index, also finding no clear trends.

We repeated the analysis using only member galaxies with $\eta < -1.4$ (non-star forming galaxies) on the one hand, and only member galaxies with $\eta > -1.4$ (star forming galaxies) on the other. Note that several groups are represented in both samples, since it is fairly common that there

will be both, star forming and non-star forming galaxies in a group. Once more, we were unable to detect any systematic differences in the shapes of groups when considering only either star forming or non-star forming galaxies. Repeating this analysis using the spectral type index in the SDSS-DR3GC catalogue produces the same results, namely, that there is no clear correlation between spectral type and group shape.

These results are somewhat surprising and indicate the need for larger samples of groups, which may provide better means to detect small differences between group shapes computed considering star forming and non-star forming galaxies separately. This could be expected, for instance, if galaxy morphological segregations in groups were to depend only on the distance to the group centre.

4 CONCLUSIONS

We have performed several analyses of shapes of gravitationally bound systems in numerical simulations, mock group catalogues, and observational group catalogues derived from the 2dFGRS and the SDSS-DR3 galaxy surveys. Our main results on the three-dimensional shapes of dark matter haloes in the numerical simulations can be summarised as follows:

• Halos are well described by triaxial ellipsoids that tend to be more prolate as the halo mass increases. This can also be detected by means of other statistical parameters; both the asphericity c/a, and the projected semi-axis ratios b/a show a clear decrement with halo mass.

• We demonstrated that low number statistics tend to bias the measured shapes toward oblate shapes. Performing a Monte-Carlo analysis, we show that the smaller semi-axes are more affected by noise, and consequently, prolate shapes, characterised by two small semi-axes, are more distorted.

Regarding the analysis of mock and real catalogues, our results can be summarised as follows:

• The analysis in redshift-space does not change significantly the distribution of projected shapes of haloes for a given distribution of group mass and number of members, although there is a weak tendency for systems in the mock catalogue to be more elongated than those obtained by direct projection of the simulations. This is probably due to differences in the identification algorithms used in simulations and redshift-space samples.

• The properties of the distribution of shapes in the mock catalogue closely resemble those in the observations, indicating the accuracy of the GALFORM model in combination with the numerical simulation to reproduce the observational data. In particular, the tendency of groups with low number of members to show elongated shapes is entirely consistent in both real and mock catalogues.

• We demonstrate that the observed trend where richer groups are rounder is an artifact of low number statistics. We provide a fit to a corrected distribution of group shapes, calibrated to match what would be obtained for a fixed $N = 20$ members.

• We also analysed subsamples of 2PIGG and SDSS-DR3GC groups selected by member galaxy colour and spectral type. We were unable to detect a significant dependence

of group shapes on fractions of red galaxies, or fractions of passively star forming galaxies.

Finally, by considering a fixed number of members per group, we were able to detect a statistically reliable trend of 2PIGG group shapes with mass (group masses are obtained via a mass-to-light ratio calibrated by Eke et al., 2004). In order to do this, we select 2PIGG groups with at least 10 member galaxies, and use only 10 randomly selected members to measure the group projected semi-axis ratios. Our findings indicate that more massive groups tend to show more elongated shapes, in excellent agreement with results from numerical simulations.

REFERENCES

Abazajian K., et al. (The SDSS Team), 2005, AJ, 129, 1755.

Colberg J.M., White S.D.M., Jenkins A., Pearce F.R., N. Yoshida, 1999, MNRAS, 308, 593

Colberg J.M., White S.D.M., MacFarland T.J., Jenkins A., Pearce F.R., Frenk C. S., Thomas P. A., Couchman H. M. P., 2000, MNRAS, 313, 229.

Cole S., Lacey C.G., Baugh C.M., Frenk C.S., 2000, MNRAS, 319, 168.

Colless M., et al. (The 2dFGRS Team), 2001, MNRAS, 328, 1029.

Cooray A., & Sheth R., 2002, Phys. Rep., 372, 1.

Eke V.R. et al. (The 2dFGRS Team), 2004, MNRAS, 348, 866

Evrard A.E., MacFarland T.J., Couchman H.M.P., Colberg J.M., Yoshida N., White S.D.M., Jenkins A., Frenk C.S., Pearce F.R., Peacock J. A., Thomas P. A., 2002, ApJ, 573, 7

Frenk C.S., White S.D.M., Davis M., Efstathiou G., 1988, ApJ, 327, 507

Hopkins P.F., Bahcall N.A., Bode P., 2005, ApJ, 618, 1.

Jenkins A., Frenk C.S., White S.D.M., Colberg J.M., Cole S., Evrard A.E., Couchman H.M.P., Yoshida N., 2001 MNRAS, 321, 372

Jing Y.P., Suto Y., 2002, ApJ, 574, 538

Kasun S.F., Evrard A.E., 2005, ApJ in press, astro-ph/0408056

Mechán M., Zandivarez A., 2005, Submitted to ApJ, astro-ph/0412257

Padilla N., & Baugh C.M., 2002 MNRAS, 329, 431.

Plionis M., Basilakos S., Tovmassian H.M., 2004, MNRAS, 352, 1323

Splinter R.J., Melott A.L., Linn A.M., Buck C., & Tinker J., 1997, ApJ, 479, 632.

Springel V., Yoshida N., White S.D.M., 2001, NewA, 6, 79

Thomas P.A., Colberg J.M., Couchman H.M.P., Efstathiou G.P., Frenk C.S., Jenkins A.R., Nelson A.H., Hutchings R.M., Peacock J.A., Pearce F.R., White S.D.M., 1998, MNRAS, 296, 1061

van den Bosch F.C., Norberg P., Mo H.J., Yang X., 2004, MNRAS, 352, 1302.

van Haarlem M., & van de Weygaert R., 1993, ApJ, 418, 544 .

Warren M.S., Quinn P.J., Salmon J.K., Zurek W.H., 1992, ApJ, 399,405